Experimental Investigation and Design Method for the Shear Strength of Self-Piercing Rivet Connections in Thin-Walled Steel Structures

Weiming Yan [1], Zhiqiang Xie [2], Cheng Yu [3], Linlin Song [4], Haoxiang He [5]

1. Professor, Beijing Key Laboratory of Earthquake Engineering and Structural Retrofit, Beijing University of Technology, Beijing, China. Yanwm@bjut.edu.cn

2. Doctoral Research Assistant, Beijing Key Laboratory of Earthquake Engineering and Structural Retrofit, Beijing University of Technology, Beijing, China. xzq198898@163.com

3. Professor, Department of Engineering Technology, University of North Texas, Denton, TX, US cheng.yu@unt.edu

4. Doctoral Research Assistant, Beijing Key Laboratory of Earthquake Engineering and Structural Retrofit, Beijing University of Technology, Beijing, China. 577070636@qq.com

5. Professor, Beijing Key Laboratory of Earthquake Engineering and Structural Retrofit, Beijing University of Technology, Beijing, China. hhx7856@163.com

ABSTRACT

The paper presents an experimental investigation on the shear strength of self-piercing rivet connections used in thin-walled steel structures. The test program included specimen variations in the number of rivets in each connection, rivet spacing, end distance, and steel sheet thickness. According to the experimental results, the curve of load-slip, peak load, and failure mechanism for all specimens were analyzed. Parameters of riveting in terms of end distance, spacing, arrangement, length, and thickness difference between connection components were studied on their effects for shearing performances of self-piercing rivet connections. A design method based on the model of transmission dynamics of infectious diseases was proposed for calculating the shear strength of the rivet connections. The strength reduction due to the effect of group rivets was considered in the new method.

Keywords*:* Self-piercing rivet, Thin-walled steel structures, Shear strength, Rivet connections, Design method

1. INTRODUCTION

Nowadays, more and more low-rise buildings adopted prefabricated cold-formed thin-walled steel structural systems [1]. In the assembling process of thin-walled structures, connections using blind rivet, clinching, welding or self-drilling screw are commonly employed [2]. The self-drilling screw is the most common type of connection in cold-formed steel structures, however the installation process can be generally complex due to the need for clamping plate, drilling, tightening screws and other steps, which may seriously reduce efficiency of industrial production for components in prefabricated cold-formed thin-walled steel structure [3]. In addition, a large number of experimental studies have found that tilting, shear and pull out of screws are the controlling failure models in cold-formed steel structures. The strength of the cold-formed steel structures is largely dependent on the shear capacity of self-tapping screws [4-5].

In order to improve the fabrication efficiency and structural reliability of cold-formed steel connections, the self-piercing rivet (SPR) technique used in the automotive industry is studied herein on cold-formed thin-walled steel structures. The process of forming SPR connection involves driving a separate rivet component into the layer of the parent metal, piercing and clinching in a single operation [2, 6, 9]. Schematic diagram of forming a SPR join is illustrated in Fig. 1. SPR has high tensile strength, shear strength, stiffness, and high efficiency in connecting steel sheets of different thickness and mechanical properties.

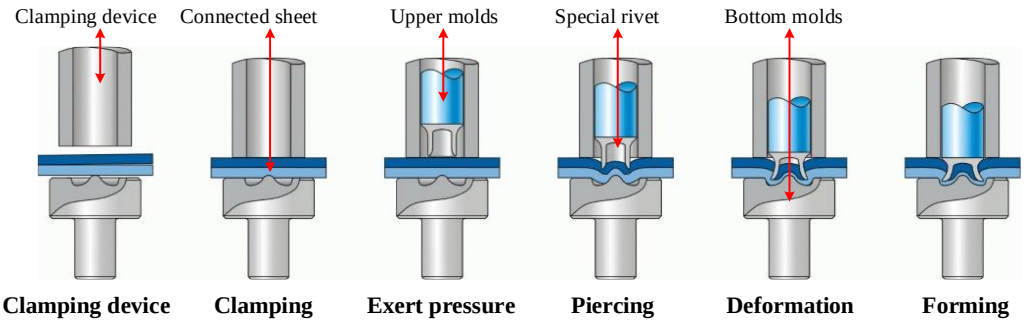

Fig. 1. Schematic diagram of the forming process of a SPR joint [10]

The previous research on SPR joints has been concentrated on the forming mechanism and fatigue behavior for ductile thick steel plates [8, 9, 11], the study on SPR connections with thin-walled steel sheets is limited. Mucha and Lennon [2, 12] studied various connections using SPRs, self-drilling screws, clinching and blind rivets. They found that SPR gave the highest stiffness and ultimate load among all investigated connection methods. Voelkner [13] suggested that the overall thickness of the connected sheets shall not be greater than 6 mm for SPR connections. Parameter analysis of SPR connections under different combinations of sheet materials was presented in Porcaro et al. [14, 15], their results suggested that thickness and material properties of sheets had significant influence on the shear strength. Li and Han [16, 17] concluded that the edge distance had effect on dynamic fatigue strength and static behavior of SPR aluminum joints.

Haque et al. [18] developed a simple model for characterizing SPR joints in steel sheets based on experimental results. Lorenzo [19] proposed a shear design formulation of the circular press-joints based on the design rules of blind rivet connections recently introduced in the European standard on cold-formed steel structures [20]. However, because of the different mechanical mechanism between the blind rivet connections and the press-joints, Lorenzo's method was not appropriate for SPR connections. LaBoube et al. [21] showed that the self-drilling screws connection had

"Group Effect", and they developed design equations to reflect the "Group Effect" on the shear strength of cold-formed steel screw connections. The previous research was mainly focused on single rivet connections. The research presented here includes both single and multiple SPR connections with cold-formed thin-walled steel. Design methods for shear strength of SPR connections using single and multiple rivets are proposed.

In this research project, a standard uniaxial shear test method was designed for specimens of single and multiple SPR connections made of cold-formed thin-walled steel sheets. Parameters in terms of end distance, number, spacing, arrangement, thickness difference between connected components and loading rate were studied on their effects for shear strength of SPR connections. Based on the transmission dynamics of infectious diseases model (SIR model), a mechanical model of single riveting was established, and then a formula of shear strength for multiple SPR connections considering the group reduction effect was developed. The research results will provide a design reference and experimental data resource for the application of SPR in the construction industry.

2. EXPERIMENTAL INVESTIGATION

2.1 The test specimens

SPR originated in Germany has become a common connection type in the automobile industry. However its application in the field of structural engineering is limited. SPR connection is currently fabricated using proprietary rivets and machines. EPRESS SYSTEMS (SHENZHEN) LTD is currently the only SPR manufacturer in China. In this paper, all the test specimens were provided by this manufacturer.

Galvanized cold-formed thin-wall steel was used in all samples. All tested samples were single shear connections consisted of two thin-walled steel sheets. The sheets were 200 mm long × 60 mm wide (Fig. 2a). Five different sheet thicknesses were investigated: 0.8-mm, 1.0-mm, 1.2-mm, 1.5-mm and 2.0-mm thick steel. Various rivet sizes were studied in the test program including diameters (*d*), length (*h*), and width (*b*) (Fig. 2b). The SPRs were made of high hardness of alloy steel, and its grade and dimensions are shown in Table 1. Tensile tests were performed on Zwick/Roell Z050 testing machine equipped with the automatic extensometer, and testing machine capacity was 50kN (Fig. 3a). The extensometer had a travel distance of 10 mm which allowed the measurement of the elastic and plastic slip in the connections (Fig. 3b). The gauge length which the elongation was measured is 100mm. The grips were pin connected to the testing machine, therefore the moment effect was eliminated when the specimen was subjected to tension forces in the tests.

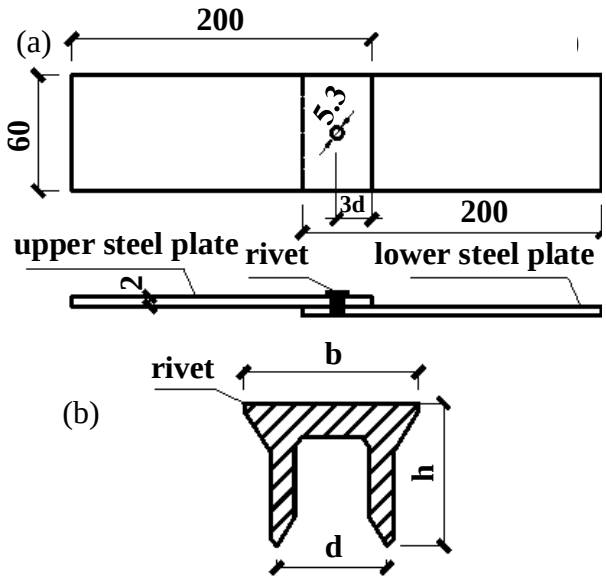

Figure 2 Dimensions of shear specimens: a) connected sheets, b) cross-section of SPR

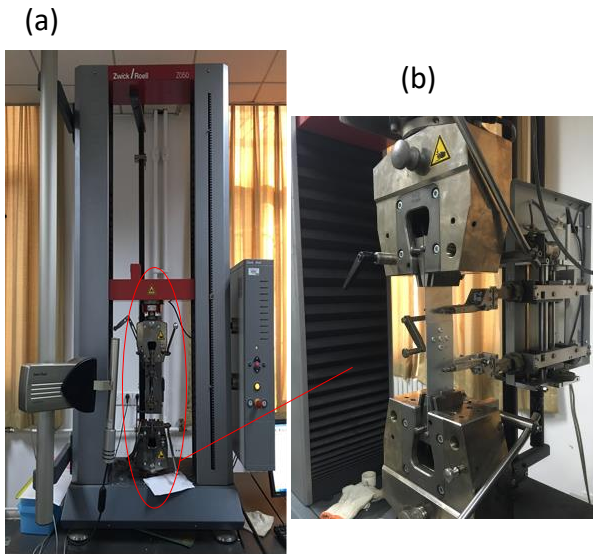

Figure 3 Test set-up: a) testing machine, b) close-up of test specimen

Table 1 Grade and dimensions for SPR

Length (mm)	Width (mm)	Diameters (mm)	Hardness (HRC)	Elastic modulus (Gpa)
4.0	7.6	5.3	40	201
4.5	7.6	5.3	45	209
5.0	7.6	5.3	44	204
5.5	7.6	5.3	46	211
6.0	7.6	5.3	42	208

SPR specimens were divided into two groups: single rivet and multiple rivets connections. Standard label format of single rivet connection specimens is illustrated in Fig. 4a. For instance, Specimen “1.2+1.5-5.3×6-5d-3”, where “1.2+1.5” represents 1.2mm thickness of upper sheet and 1.5-mm thickness of lower sheet, respectively; “5.3×6” represents rivet size, diameter of 5.3 mm, length of 6.0 mm; “5d” represents distance between center of the rivet and end of sheet (end distance) is five times of the rivet’s diameter; “3” represents loading rate is 3 mm/min. Standard label format of multiple rivet connection specimens is illustrated in Fig. 4b. For all of multiple

rivets connections, thickness of steel sheet was 1.5 mm and the end distance was five times of the rivet's diameter. For example specimen number "1.5-5-E1-N3-3d-4d", where '1.2' represents 1.2-mm steel thickness; "5" is total number of rivets; "E1" represents that number of external arrangement rivets is equal to 1; "N3" represent that number of inner arrangement rivets is equal to 3; "3d" is end distance of rivet; "4d" is rivet spacing. Specimen of five rivets is illustrated in Fig. 5.

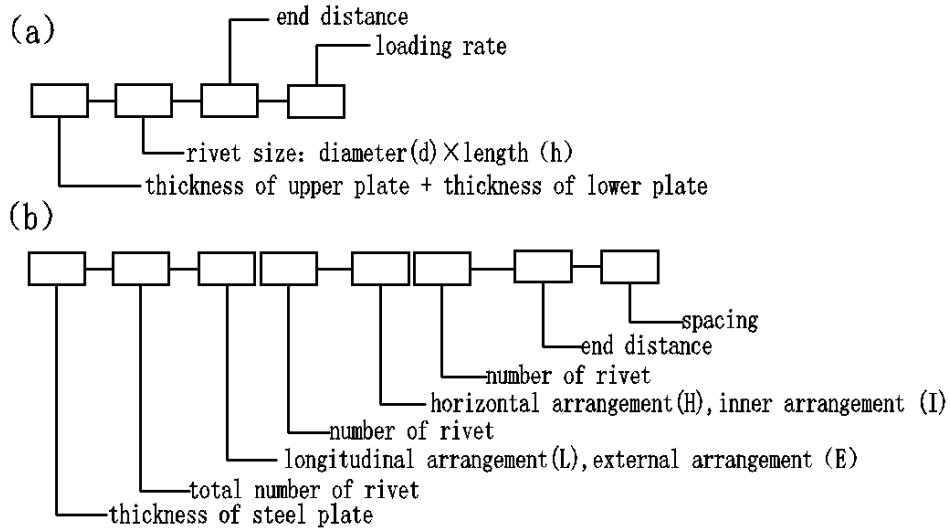

Figure 4 Standard code of test specimen: a) single rivet connection, b) multiple rivet connection

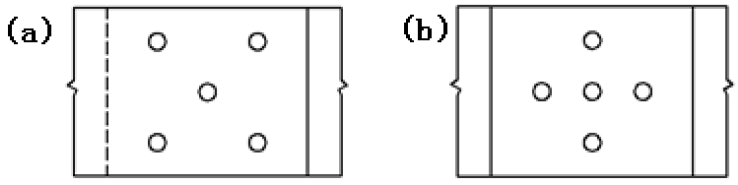

Figure 5 Specimens using five rivets: a) 1.5-5-E2-N1-3d-3d, b) 1.5-5-E1-N3-3d-3d

For each connection configuration 6 samples were tested. For clarity of achieved results of the peak load, the following equations were used to determine the average values (Eq. (1)), the standard deviation (Eq. (2)), and coefficient of variation (Eq. (3)).

$$\overline{X}_n = \frac{1}{n}\sum_{i=1}^{n} X_i \tag{1}$$

$$S = \sqrt{\frac{1}{n}\sum_{i=1}^{n}(X_i - \overline{X}_n)} \tag{2}$$

$$C_V = \overline{X}_n / S \tag{3}$$

2.2 The test specimens

Based on the Chinese Standard of Metallic Materials-Tensile Testing at Ambient Temperature (GB/T228-2002), coupon tests were conducted to obtain the actual material properties of galvanized steel sheet made of DX51D. For each thickness, 3 coupons were tested. Table 2 lists the coupon test results including the average yield strength (f_y), the average tensile strength (f_u), young's modulus (E), and tensile rate for each type of steel thickness. The nominal yield strength for DX51D steel is 235 N/mm^2, the test materials are either close or above the nominal value. The stress strain curves for the three tests of 1.5mm thickness are illustrated in Fig. 6.

Table 2 Material properties of different thickness steel sheets

Steel thickness t (mm)	Average yield strength f_y （N/mm^2）	Average tensile strength f_u （MPa）	Young's modulus E（10^5 MPa）	Tensile rate A_{80}（%）
0.8	292.0	363.7	2.00	26.6
1.0	267.7	362.0	2.05	36.0
1.2	240.7	348.7	2.17	31.4
1.5	240.3	337.7	2.10	37.4
2.0	234.3	331.3	2.12	38.3

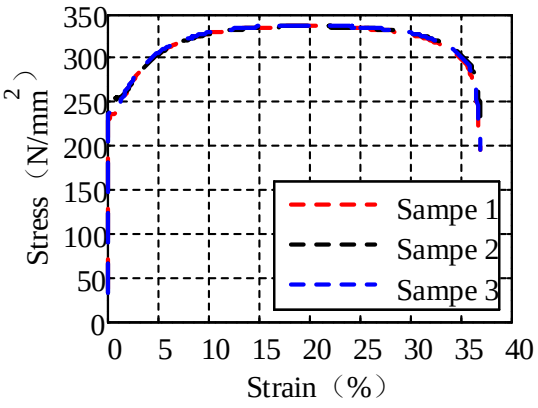

Figure 6 Stress-strain relationship for 1.5-mm thick steel

2.3 Analysis and assessment of specimens

Due to the fact that the settings in the SPR machine has significant impact to the quality of SPR connections. It is necessary to evaluate SPR connections before conducting the experiments [22]. The electronic digital microscope was employed in this research to measure the key dimensions of the cross section of SPR. As illustrated in Fig. 7, the assessment was focused on the remaining thickness, the interlock size, and the rivet opening's size.

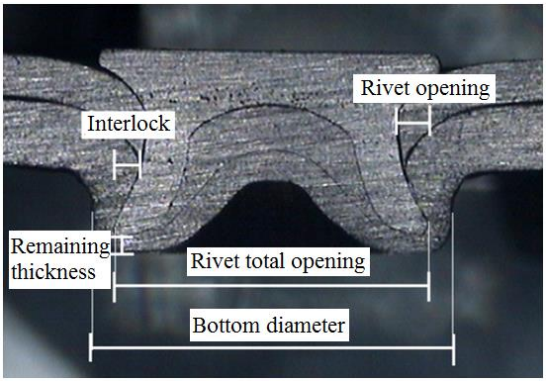

Figure 7 Typical cross section for SRP joint

At present, there are two quality evaluation methods: the visual method and the measuring method of the central section. The visual method primarily includes the observation of the surface of SPR connection (check its smoothness), the steel sheets (check the cracks), and the lower sheet whether it appears penetrating phenomenon. Measuring method of the central section is to cut the central section of joint, and measure remaining thickness, interlock size, and rivet opening and compare them with the requirements of the specified tolerance. Decreased interlock size can lead to inadequate rivet open, but the increasing of the interlock size can lead to decrease of remaining thickness. Therefore, interlock size and remaining thickness should be controlled in a relatively reasonable size range. This research recommends that the remaining thickness and interlock size should not be less than 0.2 mm and 0.3 mm, respectively.

Prior to the tests, a number of exploratory experiments were performed to evaluate the SPR connections. For each specimen configuration, 3 identical samples were fabricated and were used for qualification assessment. Table 3 lists the remaining thickness, interlock and rivet opening width for rivets under different combination of steel sheets. The research found that a qualified SPR joint shall have following characteristics: deformation of rivet is basic symmetric; rivet opening is complete; remaining thickness and interlock is greater than 0.2 mm and 0.3 mm, respectively; the upper plate does not appear cracking; the lower plate has uniform deformation, no cracks and punctured phenomenon occur. The SPR specimens used in the tests were also in conformity with the other standard of quality evaluation [23-24].

Table 3 Key parameters for SPR connections

Rivets size （mm）	Combination of steel plate（mm）	Remaining thickness （mm）	Interlock （mm）	Rivet opening （mm）
5.3×4.0	0.8+0.8	0.320	0.497	0.612
5.3×4.5	1.0+1.0	0.277	0.328	0.704
5.3×5.0	1.2+1.2	0.306	0.394	0.877
5.3×6.0	1.5+1.5	0.365	0.484	0.924
5.3×7.0	2.0+2.0	0.407	0.461	0.886
5.3×4.5	0.8+1.5	0.341	0.378	0.675
5.3×5	1.0+1.5	0.354	0.453	0.841
5.3×5.5	1.2+1.5	0.477	0.530	0.861
5.3×6	2.0+1.5	0.514	0.406	0.930

3. TEST RESULTS AND ANALYSIS

3.1 Failure modes and mechanical parameters

Yu [25] indicated that the type of failure mode influences shear capacity of the lap shear test. In cold-formed thin-walled shear connections made of SPRs, four basic types of failures could occur: (I) pull-out of rivet, (II) shear failure of the sheet steel, (III) bearing failure of the sheet, (IV) rupture of net section in the sheet. In the experiments, SPR joints could fail in a combination of those different types of failure modes. Figure 8 shows the observed failure modes in single rivet connections.

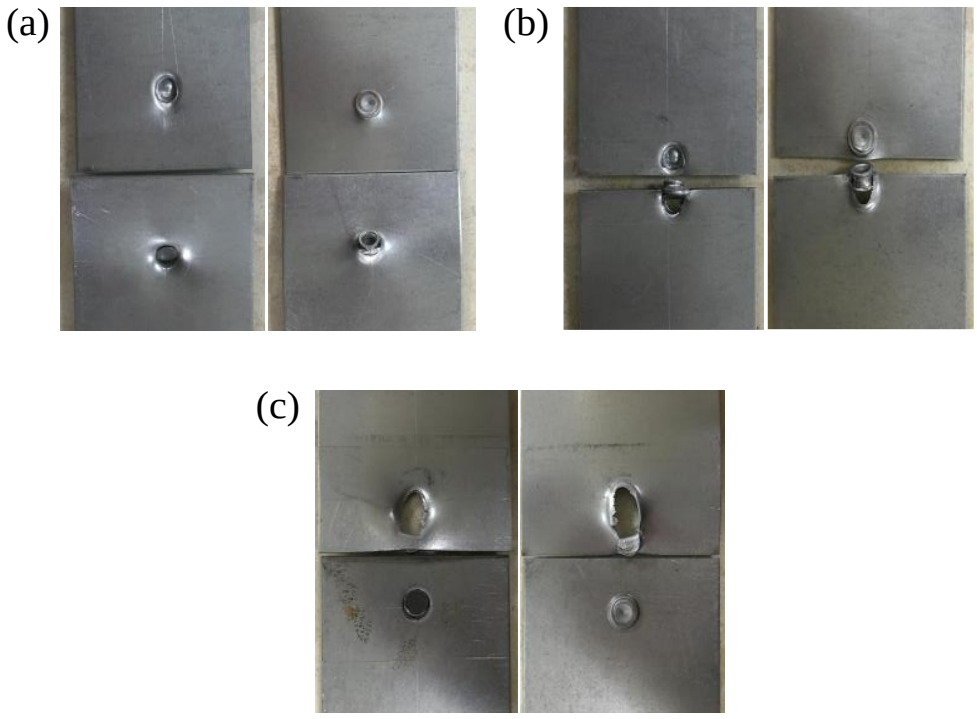

Figure 8 Failure modes of single SPR joints: a) mixed failure modes combining Type I, b) single failure mode II, c) single failure mode III

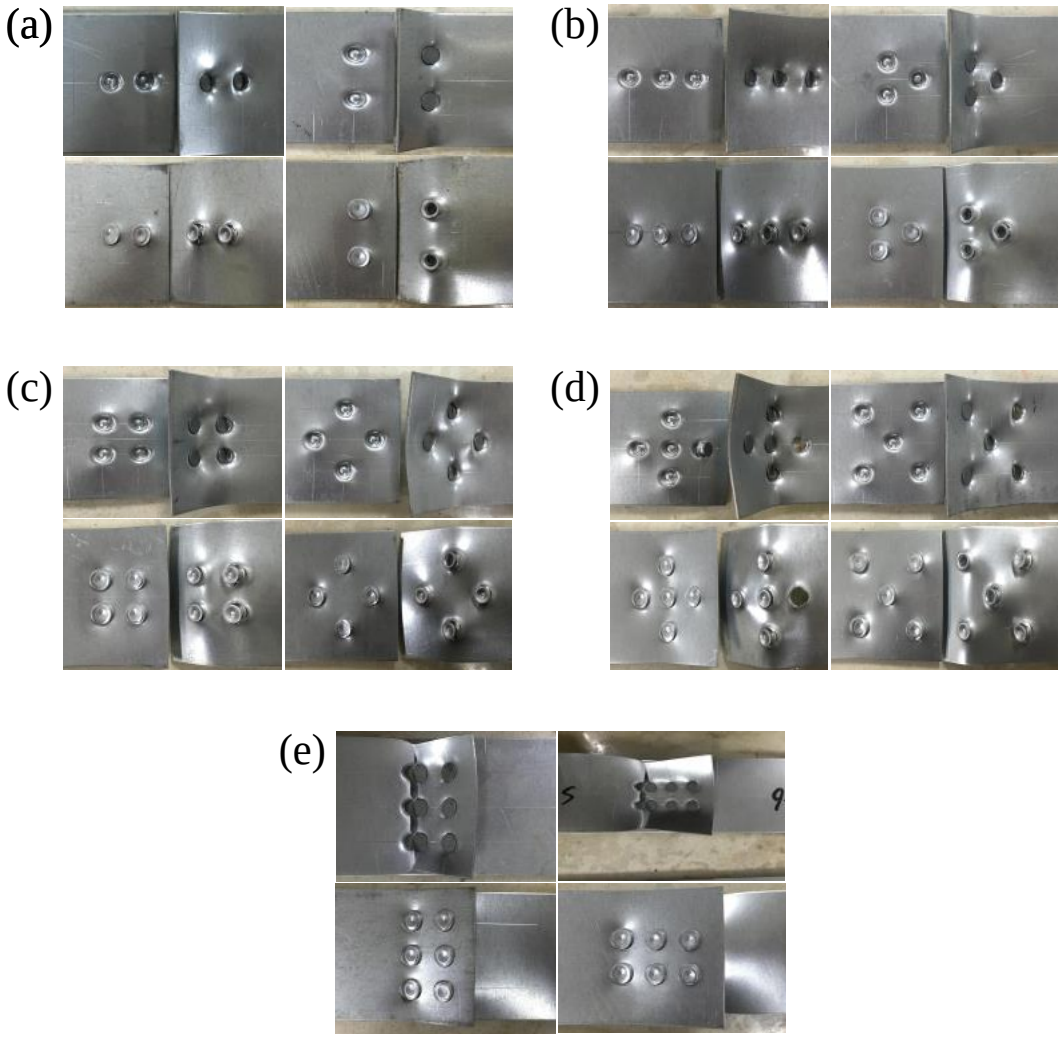

Figure 9 Failure modes of multiple SPR joint: a) - d) failure mode Type I, e) failure mode Type IV

For the multiple SPR specimens, the most common failure mode was Type I, which is illustrated in Figs. 9a to 9d. When the total shear capacity of rivets is greater than the tensile strength of steel, rupture of the sheet in net section (Type IV) occurred (Fig. 9e).

Sun and Khaleel [26] studied the dynamic strength for SPR joint made of heterogeneous sheet and they found that the dynamic strength increased with increase of loading rate. To research the

influence of loading rate against the strength of SPR connections, the tensile tests with various loading rates were done on 1.5 mm thick cold-formed thin-walled steel connections. The results are illustrated in Fig. 10. It was found that the influence of loading rate on the peak load is prominent in the range of 0.5 to 3 mm/min and 10 to 30 mm/min. When the rate is between 3 and 10 mm/min, the strength would not have significant increase. Therefore, in order to ensure the stability of the test data, the loading rate of 3 mm/min was used for this research.

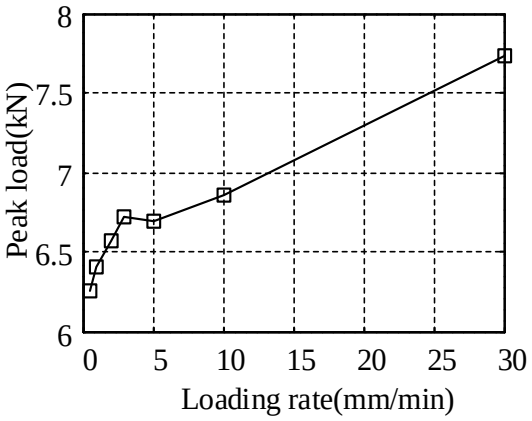

Figure 10 Loading rate-Peak load relationship for 1.5mm thick steel

Table 4 Experimental results of the tension tests

Specimen notation	Average peak load (kN)	Standard deviation	Coefficient of variation (%)	Average slip (mm)	Number of samples	Failure modes
Single rivet						
1.5+1.5-5.3×6.0-1d-3.0	4.87	0.344	7.12	0.84	6	II
1.5+1.5-5.3×6.0-2d-3.0	6.99	0.113	1.63	1.22	6	I
1.5+1.5-5.3×6.0-3d-3.0	7.41	0.246	3.38	1.15	6	I
1.5+1.5-5.3×6.0-4d-3.0	7.65	0.132	1.73	1.24	6	I
1.5+1.5-5.3×6.0-5d-3.0	7.66	0.124	1.60	1.26	6	I
1.5+1.5-5.3×5.0-3d-3.0	7.28	0.240	3.33	0.79	6	I
1.5+1.5-5.3×5.5-3d-3.0	6.81	0.370	5.42	1.17	6	I
1.5+1.5-5.3×6.0-3d-3.0	7.41	0.246	3.36	1.15	6	I
1.5+1.5-5.3×6.5-3d-3.0	7.23	0.288	4.06	1.37	6	I
1.5+1.5-5.3×7.0-3d-3.0	7.33	0.252	3.40	2.60	6	I
0.8+0.8-5.3×4.0-3d-3.0	3.57	0.093	2.60	1.02	6	I
1.0+1.0-5.3×4.5-3d-3.0	4.59	0.110	2.46	1.06	6	I
1.2+1.2-5.3×5.0-3d-3.0	6.31	0.038	0.69	1.12	6	I
2.0+2.0-5.3×7.0-3d-3.0	9.39	0.095	1.00	1.91	6	I
0.8+1.5-5.3×4.5-3d-3.0	4.39	0.099	2.30	1.18	6	III
1.0+1.5-5.3×5.0-3d-3.0	5.42	0.104	1.94	1.72	6	I+III
1.2+1.5-5.3×5.5-3d-3.0	6.55	0.206	3.17	1.54	6	I
1.5+2.0-5.3×6.5-3d-3.0	7.68	0.156	2.01	0.72	6	I
Multiple rivets						
1.5-2-L1-H2-3d-2d	13.00	0.118	0.91	1.33	6	I
1.5-2-L1-H2-3d-3d	13.29	0.169	1.26	1.33	6	I
1.5-2-L1-H2-3d-4d	13.88	0.098	0.71	1.29	6	I
1.5-2-L1-H2-3d-5d	14.07	0.085	0.60	1.21	6	I
1.5-2-L1-H2-3d-6d	14.06	0.222	1.58	1.18	6	I
1.5-2-L1-H2-3d-7d	13.78	0.167	1.21	1.09	6	I
1.5-2-L2-H1-3d-2d	13.29	0.219	1.65	1.31	6	I
1.5-2-L2-H1-3d-3d	13.92	0.202	1.45	1.35	6	I
1.5-2-L2-H1-3d-4d	14.43	0.072	0.50	1.40	6	I
1.5-2-L2-H1-3d-5d	14.66	0.151	1.03	1.48	6	I
1.5-2-L2-H1-3d-6d	14.96	0.213	1.43	1.16	6	I
1.5-2-L2-H1-3d-7d	15.05	0.256	1.69	1.21	6	I
1.5-3-L1-H3-3d-3d	18.14	0.163	0.90	1.38	6	I
1.5-3-L3-H1-3d-3d	19.15	0.156	0.82	1.83	6	I
1.5-3-E2-E1-3d-3d	18.32	0.281	1.54	1.68	6	I
1.5-4-L2-H2-3d-3d	20.99	0.174	0.83	2.26	6	I
1.5-4-E1-N2-3d-3d	24.15	0.162	0.67	4.04	6	I
1.5-5-E2-N1-3d-3d	28.26	0.208	0.73	6.53	6	I
1.5-5-E1-N3-3d-3d	25.64	0.134	0.52	4.60	6	I
1.5-6-L2-H3-3d-3d	25.69	0.151	0.59	4.01	6	IV
1.5-6-L3-H2-3d-3d	26.69	0.112	0.42	4.37	6	IV

The test results are summarized in Table 4. The strength parameter assumed to characterize the shear capacity of each connection is the peak load (P_u). With regard to the ductility parameter, the slip (ε) achieved in correspondence of the peak load P_u has been used. In Table 4, all the

mechanical parameters provided by the shear behavior of SPR connections, together with the actual failure modes, are reported.

The test specimens included connections with different thicknesses. It was found that when the thickness of bottom sheet was fixed, the peak load of SPR connection decreased with increase of thickness difference between the bottom (thicker) and upper (thinner) sheets. The thickness difference was the most critical factor that affected the failure mechanism and mechanical properties of SPR connections. The thickness ratio between thick sheet and thin sheet should not be greater than 1.5 in order to assure satisfied performance. The test specimens also included connections with different rivet lengths. It was found that the rivet length did not impact the peak load, however it did affect the failure mode.

3.2 Analysis of the experimental results

Table 4 shows that the rivet pull-out failure (Type I) and net section rupture (Type IV) are the main failure modes of all shear specimens. The interpretation of experimental results is based on the load- slip response of typical shear specimens (Fig. 10). With regard to typical shear specimens of Type I failure mode, the curve of load-slip can be divided into four stages: elastic stage (linear relationship between load and slip), elastic-plastic stage (nonlinear slow increase relationship between load and slip), plastic stage (nonlinear slow decrease relationship between load and slip), failure stage (sharply decrease relationship between load and slip) (Fig. 11a). However, with regard to typical Type IV failure mode (Fig. 11b), the typical load-slip curve is only divided into three stages and lack of the plastic stage. In particular, as far as the ductility is concerned, the analysis of the test results indicates that the specimens of Type I failure mode provides better ductility performances than specimens of Type IV failure mode.

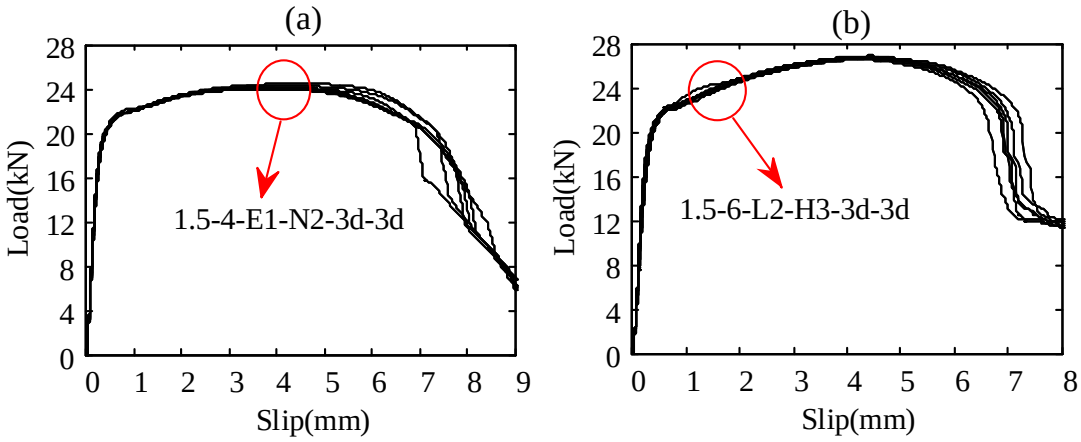

Figure11 Load-slip response of typical shear specimens of main failure mode: a) failure mode Type I, b) failure mode IV

3.3 Effect of rivet end distance

The test specimens that the specimen notation was 1.5+1.5-5.3×6.0-*X*-3.0 were performed for 5 different rivet end distance, *X*=1*d*, 2*d*, 3*d*, 4*d*, 5*d*. The effect of the rivet end distance on the peak load is illustrated in Fig. 12. It shows that the peak load reduces with the decrease of rivet end distance. The reduction in load is significant for specimens with end distance less than 3 times of the diameter of rivet. When the end distance is within 3-5 times of the rivet's diameter, the influence on the peak load is limited. In order to ensure the reliability of SRP connections, the end distance should not be less than 3 times of the rivet's diameter.

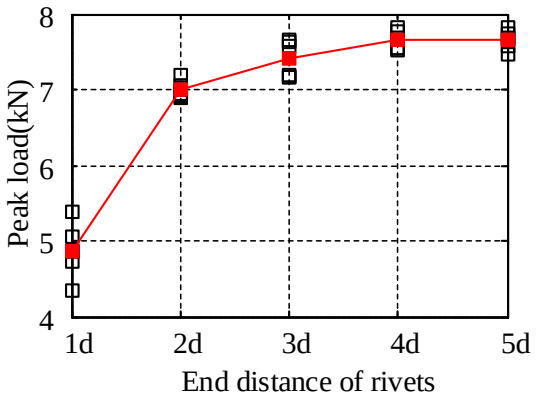

Figure12 End distance of rivets-Peak load relationship for 1.5 mm thick steel

3.4 Effect of rivet spacing

The test specimens with notations of 1.5-2-L1-H2-3d-*X* and 1.5-2-L2-H1-3d-*X* were performed for 7 different rivet spacing, *X*=1*d*, 2*d*, 3*d*, 4*d*, 5*d*, 6*d*, 7*d*. Relationship between peak load and spacing for two rivet orientation arrangements (horizontal and longitudinal to the loading) is illustrated in Fig. 13. Fig. 13 shows that peak load increases with increase of the rivet spacing. However, when the rivet spacing is more than four times of the diameter of rivet, the increase is not significant. Fig. 13 also shows that peak load of the specimens with longitudinal arrangement is greater than that with the horizontal arrangement. Therefore, in order to ensure the reliability of SPR connections, the spacing of rivets should not be less than 4 times of the rivet's diameter.

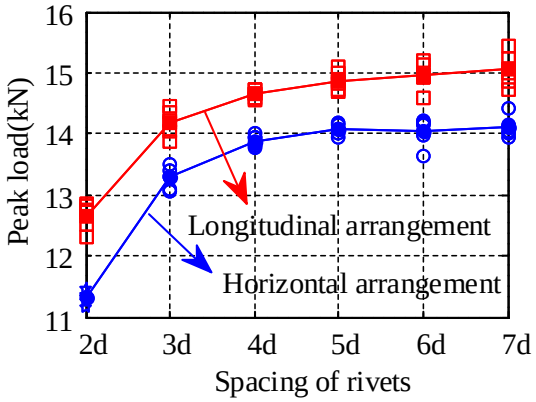

Figure 13 Spacing of rivets-Peak load relationship for 1.5 mm thick steel

3.5 Effect of rivet arrangement and number

Comparison of shear capacity of specimens with regard to the number of rivets is listed in Table 5. In Table 5, P_u is the peak load of specimen; P_1 is the peak load of single rivet specimen; $\bar{P}$ is the equivalent ultimate shear capacity per rivet, which is defined as P_u / n where n refers to the number of rivets. Table 5 shows that the orientation of rivets has a significant influence on peak load. For the connections with the same number rivets, the longitudinal arrangement (rivet line parallel to the force direction) gave the highest strength, the horizontal arrangement gave the lowest strength, and the hybrid arrangement yielded an intermediate level strength. The tests show significant reduction effect of group rivets, and the equivalent ultimate shear capacity per rivet consistently decreases with increase of the number of rivets.

Table 5 Effect of arrangement and number of rivet on shear capacity

Number of rivets	Specimen notation	P_u(kN)	P / P_1	$\bar{P}$(kN)
1	1.5+1.5-5.3×6.0-3d	7.41	1	7.41
2	1.5-2-L1-H2-3d-3d	13.29	1.79	6.65
	1.5-2-L2-H1-3d-3d	13.92	1.88	6.96
3	1.5-3-L1-H3-3d-3d	18.14	2.45	6.05
	1.5-3-L3-H1-3d-3d	19.15	2.58	6.38
	1.5-3-E2-E1-3d-3d	18.32	2.47	6.11
4	1.5-4-L2-H2-3d-3d	20.99	2.83	5.25
	1.5-4-E1-N2-3d-3d	24.15	3.30	6.03
5	1.5-5-E2-N1-3d-3d	28.26	3.81	5.65
	1.5-5-E1-N3-3d-3d	25.64	3.46	5.13

4. PREDICTION METHOD OF SHEAR STRENGTH

4.1 Predicting the Shear Strength of single SPR connection

Due to the complex mechanics mechanism and major influence factors of shear capacity, a simple linear formula could not be used to describe the relationship between load and slip for the SPR connections. Based on the transmission dynamics model of infectious diseases (SIR model) [27, 28], a stress-strain model for SPR specimens was established to account for SPR behaviors:

$$\begin{cases} \dfrac{d\sigma}{d\varepsilon} = \lambda\sigma s - \mu\sigma \\ \dfrac{ds}{d\varepsilon} = -\lambda\sigma s + \eta\sigma - \rho\sigma^2 s \end{cases} \tag{4}$$

Where ε is effective slip of element; $s(\varepsilon)$ and $\sigma(\varepsilon)$ are equivalent stress for undeformed element and deformed element, respectively; $r(\varepsilon)$ is equivalent stress of failure element, and it is reserved for $s(\varepsilon)+\sigma(\varepsilon)+r(\varepsilon)=1$. λ is the stress transfer rate of element; μ refers to failure rate of element; η is the increasing rate of stressed element; and ρ is the reduced velocity parameter of failure element.

As a nonlinear differential equations group, Equations (4) have a unique solution, but the general mathematical method cannot get its analytical solution. Therefore, the numerical calculation method is usually used to solve it. In this paper, based on the homotopy analysis method (HAM) [27-29], approximate analytic solution of Formula (4) is derived in Formula (5):

$$\begin{cases} \sigma(\varepsilon) = \sum\limits_{m=1}^{+\infty}\sum\limits_{k=1}^{3m+2} \delta_{m,k} e^{-k\theta\varepsilon} \\ s(\varepsilon) = s(0) + \sum\limits_{m=1}^{+\infty}\sum\limits_{k=1}^{3m+2} \eta_{m,k} e^{-k\theta\varepsilon} \end{cases} \tag{5}$$

Where $\theta = \mu - \lambda s(\infty) \approx \mu$ is assumed; m, δ, θ, η and k is coefficient.

According to characteristic of analytic solution, Formula (5) can be simplified:

$$\sigma = \sum_{i=1}^{n} (-1)^{i+1} c_i e^{-k_i \mu \varepsilon} \tag{6}$$

Where n is even number, and in general, c_i is equal to c_{i+1} when i is an odd number; k is coefficient.

On that basis, so for n = 2， stress - strain model for single rivet connection is obtained：

$$\sigma = \gamma (e^{\alpha \varepsilon} - e^{\beta \varepsilon}) f \tag{7}$$

In order to consider dimension parameters for single SPR connection, the following load - slip mechanical model is proposed:

$$F_1 = \xi t_1 d \gamma \left(e^{\alpha t_1 \varepsilon} - e^{\beta d \varepsilon} \right) f \tag{8}$$

where F_1 and ε are the ultimate shear strength (N) and slip (mm) for single rivet connections, respectively; t_1 and t_2 are the thickness for thin sheet and thick sheet (mm), respectively; d is the diameter of rivet (mm); f is the ultimate tensile strength of the sheet material (N/mm^2); α, β and γ are parameters reflecting properties of SPR connections, which are calculated and determined by a curve fitting method in MATLAB [30]; ξ refers to coefficient of correction considering length of rivet having effect on shear strength.

Figure 14 shows the comparison between the fitting curves and the test results for different thicknesses. Based on the SIR model, a mechanics model of SPR is proposed, which is able to present reasonably the trend for the load - slip curves in both the elastic and plastic stages.

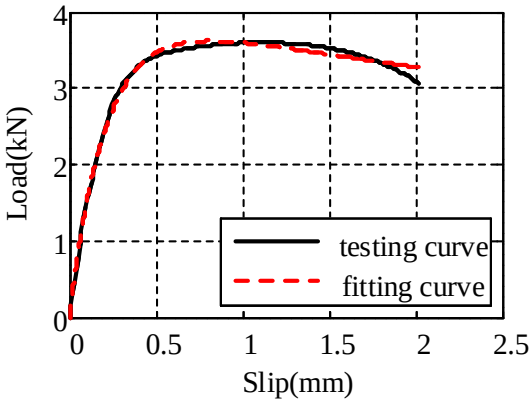

（a）S0.8+S0.8

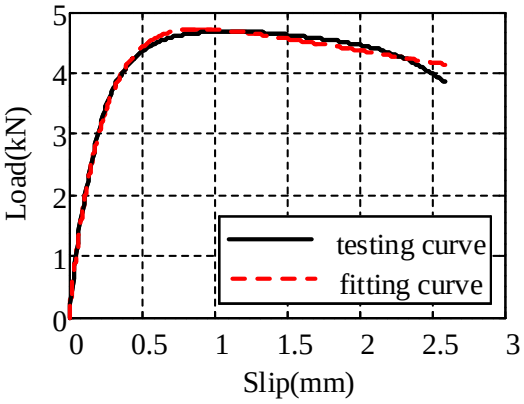

（b）S1.0+S1.0

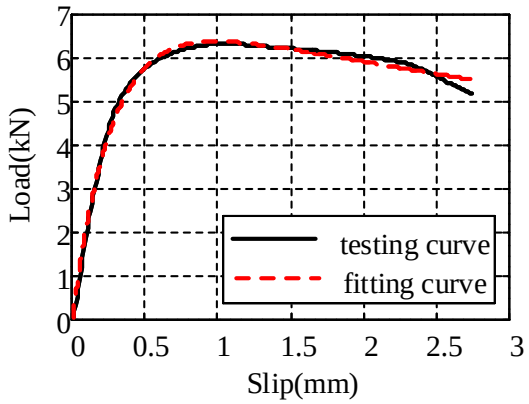

（c）S1.2+S1.2

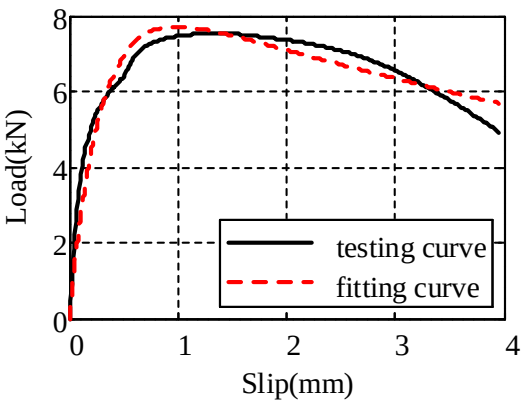

（d）S1.5+S1.5

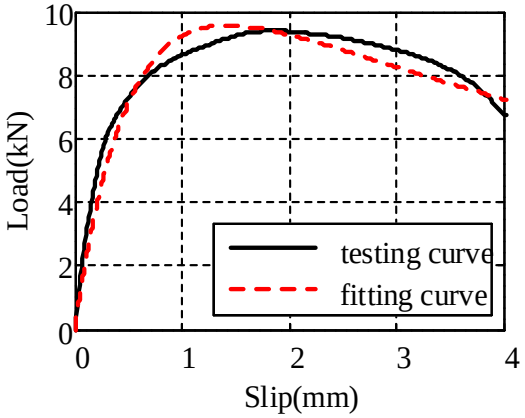

（e）S2.0+S2.0

Figure 14 Comparison between fitting curves and test results

For $t_2/\ t_1 = 1$, the values for α, β and γ are listed in Table 6 under different combination of thicknesses. t_1 is the thickness of top sheet, t_2 is the thickness of bottom sheet.

For $1 < t_2/\ t_1 \leqslant 1.5$

$$\alpha = (\alpha_i+\alpha_j)/2,\ \beta = (\beta_i+\beta_j)/2,\ \gamma = (\gamma_i+\gamma_j)/2 \tag{9}$$

Where α_i, β_i and γ_i are parameters for the thickness combination of $t_1 + t_1$ in Table 6; α_j, β_j and γ_j are parameters for the thickness combination of $t_2 + t_2$ in Table 6. According to analysis of the test data, the value of ξ is equal to 0.9 in this case. ε is deduced by F_1' (the derivative of F_1) assumed equal to zero, then by plugging ε into Equation (8); the equation for calculating the nominal shear strength of single rivet connection can be obtained as follows.

$$F_{1\max} = \xi t_1 d\gamma\left(e^{\alpha t_1\left(\frac{\ln|\beta d|-\ln|\alpha t_1|}{\alpha t_1-\beta d}\right)} - e^{\beta d\left(\frac{\ln|\beta d|-\ln|\alpha t_1|}{\alpha t_1-\beta d}\right)}\right) f \tag{10}$$

Table 6 lists a comparison between the test values and the theoretical values for individual single rivet connections under different combination of thicknesses. Test results are in a good agreement with the predicted values, and the deviation is within 6%. Table 7 provides an overall statistical analysis for the single rivet connections.

Table 6 Comparison between the test results and the predicted strength for single rivet connections

Combination of thickness (mm)	α	β	γ	Test results (kN)	Predicted strength (kN)	Deviation (%)
0.8+0.8	-0.127	-0.911	2.603	3.57	3.62	1.30
1.0+1.0	-0.090	-0.813	2.730	4.59	4.72	2.97
1.2+1.2	-0.082	-0.710	3.245	6.31	6.36	0.77
1.5+1.5	-0.076	-0.673	3.331	7.41	7.71	4.14
2.0+2.0	-0.067	-0.382	3.539	9.39	9.56	1.82
0.8+1.5	-0.102	-0.832	2.967	4.39	4.17	5.11
1.0+1.5	-0.083	-0.743	3.031	5.42	5.24	3.27
1.2+1.5	-0.079	-0.692	3.288	6.55	6.45	1.55
1.5+2.0	-0.072	-0.528	3.435	7.68	7.63	5.62

Table 7 Statistical results of the test-to-predicted ratio for single rivet connections

Test of number	Average values	Standard deviation	Coefficient of variation (%)
54	1.00	0.03	3.00

4.2 Predicting the Shear Strength of multiple SPR connections

The reduction effect of group rivets shall be considered in the design method. Effective coefficient of single rivet can be defined by Eq. (11):

$$\overline{R}=\overline{P}/P_1 \tag{11}$$

Where $\overline{R}$ is effective coefficient of single rivet; $\overline{P}$ is refers to is the equivalent ultimate shear capacity per rivet; P_1 is the peak load of single rivet specimen.

Relationships between the effective coefficient of single rivet and the number of rivets are fitted by using test data for the horizontal arrangement of rivets. Fig. 14 is a graphic presentation of 'reduction effect of group rivets' by comparing the test data with LaBoube's model [21] and the model proposed in this research. The model proposed in research, Eq. (12), is approximating the

bottom boundary of the test data, and it gives appropriate and conservative predictions for the group effect.

$$R = 0.58 + 0.42/\sqrt{n} \le 1 \tag{12}$$

Where R is the reduction factor of group rivets from the fitting results; n is number of rivets.

As shown by Fig. 15, when $n \le 5$, the proposed model can appropriately present test data for different end distance and spacing.

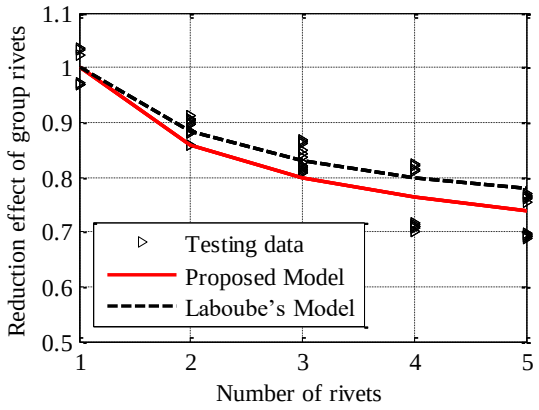

Figure 15 Reduction effect of group rivets versus number of rivets

The design of shear strength of multiple rivet connections can be expressed as:

$$F_{max} = nRF_{1max} \tag{13}$$

Where F_{max} is the nominal shear strength for specimens; n is number of rivets; R is the reduction coefficient of group rivets; F_{1max} is the nominal shear strength for single rivet specimens. The comparison between the test results and the proposed design method is provided in Tables 8 and 9.

Table 8 Comparison between the test results and the predicted strength for multiple rivet connections

Specimen notation	α	β	γ	Test results (kN)	Predicted strength values (kN)	Deviation (%)
1.5+1.5-5.3×6.0-3d-3.0	-0.076	-0.673	3.331	7.41	7.71	3.89
1.5-2-L1-H2-3d-3d	-0.076	-0.673	3.331	13.29	13.52	1.70
1.5-3-L1-H3-3d-3d	-0.076	-0.673	3.331	18.14	19.02	4.63
1.5-4-L2-H2-3d-3d	-0.076	-0.673	3.331	20.99	24.36	13.83
1.5-5-E1-N3-3d-3d	-0.076	-0.673	3.331	25.64	29.60	13.38

Table 9 Statistical results of the test-to-predicted ratio for multiple rivet connections

Test of number	Average values	Standard deviation	Coefficient of variation (%)
30	0.93	0.06	6.00

Comparison between the proposed design method with the existing test results from other researchers [2, 19, 31] is provided in Table 10. Table 10 show that proposed method is in good agreement with the others' test data, and deviation is within 7%. The shear strength of multiple SPR connections can be predicted appropriately by Eq. (13).

Table 10 Comparison between the test values in [2, 19, 31] and the theoretical values

Thickness (mm)	Lennon [2] (kN)	Theoretical values(kN)	Deviation (%)	Moss [31] (kN)	Theoretical values(kN)	Deviation (%)	Lorenzo [19] (kN)	Theoretical values(kN)	Deviation (%)
0.8+0.8	--	--	--	4.77	4.48	6.19	--	--	--
1.0+1.0	5.28	5.10	1.70	5.93	5.87	1.01	--	--	--
1.2+1.2	6.17	6.36	2.98	6.78	6.56	3.23	--	--	--
1.6+1.6	8.90	8.72	2.04	--	--	--	--	--	--
2.0+2.0	11.11	10.04	6.36	--	--	--	10.16	10.21	0.45

4.3 Predicting the Shear Strength of multiple SPR connections

For the proposed shear strength methods, the resistance factors, ϕ, for Load Resistance Factor Design (LRFD) and the safety factor, Ω, for the Allowable Strength Design (ASD) were

determined in accordance with Chapter K of AISI S100 [32]. The resistance factors, ϕ, can be determined by the Equation 14.

$$\phi = C_{\phi}(M_m F_m P_m)e^{-\beta\sqrt{V_M^2 + V_F^2 + C_P V_P^2 + V_Q^2}} \quad (14)$$

where:C_{ϕ} =calibration coefficient (1.52 for LRFD);

M_m = mean value of material factor;

F_m = mean value of fabrication factor;

P_m = mean value of professional factor;

β = target reliability index (3.5 for LRFD);

V_M =coefficient of variation of material factor;

V_F = coefficient of variation of fabrication factor;

C_p = coefficient factor;

V_P = is coefficient of variation of test results;

V_Q = coefficient of variation of load factor (0.21 for LRFD).

The values of M_m, V_M, F_m, and V_F, were taken from Table K2.1.1-1 in AISI S100 [32]. The safety factor for ASD design can be determined by the Equation 15.

$$\Omega = 1.6/\Phi \quad (15)$$

Table 11 summarizes the calculated resistance factors and safety factors as well as the other factors adopted in the calculation.

Table 11 Resistance factor and safety factor calculations

Type of data	Shear design for single rivet connection (Eq. 10)	Shear design for multiple rivet connection (Eq. 13)
Quantity	54	30
Mean	1.00	0.93
Std. Dev.	0.03	0.06
COV	0.03	0.06
M_m	1.10	1.10
V_m	0.10	0.10
F_m	1.00	1.00
P_m	1.00	0.93
V_f	0.15	0.15
B (LRFD)	3.5	3.5
V_Q	0.21	0.21
ϕ (LRFD)	0.62	0.57
Ω (ASD)	2.60	2.80

5. CONCLUSIONS

To introduce technology of SPR rivet connection to the cold-formed thin-walled steel structures, a test program was designed and conducted on both single and multiple SPR connections. Parameters in terms of end distance, spacing, number, arrangement, rivet length, thickness difference between connection components and ratio of loading were studied for their effects on the shear strength of SPR connections. Mechanical model of single riveting connection is established, and the reduction effect of group rivets is proposed for predicting the nominal shear strength for multiple rivet connections. The following conclusions can be drawn:

1. The main failure mode of SPR joint is ductile failure with pull-out of the revit.

2. In order ensure satisfied performance, the thickness ratio between thick sheet (bottom) and thin sheet (top) should not be greater than 1.5.

3. For effecting failure mechanism and mechanical properties of SPR joint, the end distance is a major factor. The shear strength increases with the increase of end distance, after more than three times diameter of rivet, its rate of gain is not obvious.

4. For certain number and arrangement of rivets, the shear strength of SPR joint increases with the increase of spacing, after more than four times diameter of rivet, its rate of gain is not obvious.

5. The orientation of rivets has significant influence on shearing strength of SPR joint. The longitudinal arrangement (along direction of force) has higher strength than the hybrid arrangement and the horizontal arrangement. The horizontal arrangement gave the lowest strength.

6. Relation between shear strength and number of rivets is out of all proportion, which is obvious "reduction effect of group rivets", and that equivalent shearing strength of single rivet joint decreases with increase of number of rivets.

7. Based on the transmission dynamics of infectious diseases model (SIR model), mechanics model of single SPR joint is proposed, which is able to present accurately change the trend for curve of load - slip. The proposed formulae can appropriately predict the nominal shear strength of SPR joint.

8. Reduction in connection strength due to the group effect was considered in the proposed nominal shear strength of multiple SPR joints.

9. LRFD resistance factor and ASD safety factor were computed according to AISI S100.

ACKNOWLEDGEMENTS

The authors would like to recognize the support by the Academic Innovation Team Program of the Earthquake Resistance and Shock Absorption of the Chinese Education Ministry. This research was also co-funded by the Innovative Research Team and the Faculty Career Development Program of Beijing Municipal Education Commission. The technical advising provided by ERPESS Systems (Shenzhen) Ltd is highly appreciated.

REFERENCES

[1] Hancock GJ. Cold-formed steel structures, Journal of Constructional Steel Research. 59 (4) (2003) 473-487.

[2] Lennon R, Pedreschi R, Sinha BP. Comparative study of some mechanical connections in cold formed steel, Construction and Building Materials. 13 (99) (1999) 109-116.

[3] Davies JM. Recent research advances in cold-formed steel structures, Journal of Constructional Steel Research. 55 (1-3) (2000) 267-288.

[4] Toma A, Sedllacek G, Weyand K. Connections in cold-formed steel, Thin Walled Struct. 16 (1-4) (1993) 219-237.

[5] Serrette R, Peyton D. Strength of screw connections in cold-formed steel construction, Journal of Structural Engineering. 135 (8) (2009) 951-958.

[6] He X, Pearson L, Young K. Self-pierce Riveting for sheet Materials: State of the Art, Journal of Materials Processing Technology. 199 (1/3) (2008) 27-36.

[7] Fiore V, Alagna F, et al. Effect of curing time on the performances of hybrid/mixed joints, Journal of Constructional Steel Research. 45 (1) (2013) 911-918.

[8] Xing BY, He XC, Zeng K, et al. Mechanical properties of self-piercing riveted joints in

alumium alloy 5052, International Journal of Advanced Manufacturing Technology. 75 (1-4) (2014) 351-361.

[9] Mori.K, Abe Y, Kato T. Self-pierce riveting of multiple steel and aluminium alloy sheets, Journal of Materials Processing Technology. 214(10) (2014) 2002-2008.

[10] Product brochure, EPRESS STSTEMS (ShenZhen) LTD, China. 2016.

[11] Hoang N-H, Porcaro R, Langseth M, Hanssen A-G, Self-piercing riveting connections using aluminium rivets, Int J Solids Struct. 47 (2010) 427–439.

[12] Jacek Mucha, Waldemar Witkowski. The experimental analysis of the double joint type change effect on the joint destruction process in uniaxial shearing test, Thin-Walled Structures. 66 (2013) 39-49.

[13] Voelkner W. Present and future developments of metal forming: selected examples, Journal of Materials Processing Technology. 106 (1-3) (2000) 236-242.

[14] Porcaro R, Hanssen AG, Langseth M. Self-piercing riveting process: an experimental and numerical investigation, Journal of Materials Processing Technology. 171 (1) (2006) 10-20.

[15] Porcaro R, Hanssen AG, Langseth M. The behaviour of a self-piercing riveted connection under quasi-static loading conditions, International Journal of Solids and Structures. 43 (17) (2006) 5110-5131.

[16] Li D, Han L, Thornton M, Shergold M. Influence of edge distance on quality and static behaviour of self-piercing riveted aluminium joints, Materials & Design. 34(2012) 22-31.

[17] Li D, Han L, Thornton M, Shergold M. Influence of rivet to sheet edge distance on fatigue strength of self-piercing riveted aluminium joints, Materials Science and Engineering: A. 558 (2012) 242-252.

[18] Rezwanul Haque, Williams Neal S, ea tl. A simple but effective model for characterizing

SPR joints in steel sheet, Journal of Materials Processing Technology. 223 (2015) 225-231.

[19] Di Lorenzo G, Landolfo R. Shear experimental response of new connecting systems for cold-formed structures, Journal of Constructional Steel Research. 60 (3-5) (2004) 561-579.

[20] CEN, prEN1993-1-3. Eurocode 3: design of steel structures-Part 1-3: general rules-supplemen-tary rules for cold formed thin gauge members and sheeting (2nd Draft), 2002.

[21] LaBoube RA, Sokol MA. Behavior of screw connections in residential construction, Journal of Structural Engineering. 128 (1) (2002) 115-118.

[22] Landolfo R, Di Lorenzo G, Fiorino L. Attualità e prospettive dei sistemi costruttivi cold-formed, Costruzioni Metalliche. 1(2002) 33-50 (in Italian).

[23] Han L, Chrysanthou A. Evaluation of quality and behaviour of self-piercing riveted aluminium to high strength low alloy sheets with different surface coatings, Materials and Design. 29 (2008) 458-468.

[24] He X C，Xing B Y，Zeng K，et al. Numerical and experimental investigations of self-piercing riveting, The International Journal of Advanced Manufacturing Technology. 69 (1-4) (2013) 715-721.

[25] Yu WW. Cold formed design, 3rd ed. New York: John Wiley & Son. 2000.

[26] Sun X, Khaleel M A. Dynamic strength evaluations for self-piercing rivets and resistance spot welds joining similar and dissimilar metals, International Journal of Impact Engineering. 34 (10) (2007) 1668-1682.

[27] Haoxiang HE, Enzhen Han, Maolin Cong. Constitutive Relation of Engineering Material Based on SIR Model and HAM, Journal of Applied Mathematics (2014), http://dx.doi.org/10.1155/2014/624863.

[28] Griffiths J, Lowrie D, Williams J. An age-structured model for the AIDS epidemic,

European Journal of Operational Research. 124 (1) (2000) 1-14.

[29] Jafari H, Das S, Tajadodi H. Solving a multi-order fractional differential equation using homotopy analysis method, Journal of King Saud University-Science. 23 (2) (2011)151-155.

[30] MATLAB R2016b, The MathWorks, Inc., Natick, Massachusetts, United States.

[31] Moss S, Mahendran M. Structural Behaviour of Self-piercing Riveted Connections in Steel Framed Housing, Sixteenth International Specialty Conference on Cold-Formed Steel Structures. 16 (2002) 748-762.

[32] AISI S100 North American Specification for the Design of Cold-Formed Steel Strutural Members, 2016 Edition, American Iron and Steel Institute, Washington, DC.